A Numerical Technique for Simulating Random Fields

A. Oya, J. Navarro-Moreno, J.C. Ruiz-Molina and R.M. Fernández-Alcalá *

Abstract—**A unified technique for generating homogeneous/non-homogeneous, Gaussian/non-Gaussian random fields defined on any subset of the multidimensional Euclidean space is provided. This is based on an approximate series representation valid for spatial random fields with arbitrary covariance function which can be readily realized. Furthermore, its applicability as a simulation tool is examined numerically by considering some examples that illustrate its feasibility and accuracy.**

Keywords: random field, Rayleigh-Ritz method, series representation, simulation

1 Introduction

In several fields of engineering, such as soil mechanics, hydrological engineering, mechanical engineering, earthquake engineering, structural engineering and many others, it is usual to model uncertainties in physical phenomena through spatial random fields (SRF) reflecting the spatial variation of the natural process [1]-[2]. In this sense the availability of a suitable procedure for generating realizations of the particular random model can be a key question for the analysis of the structural properties of the natural phenomenon under study. In fact, the simulation of SRF is a widely used tool and different methods have already been proposed, often based on the spectral representation of the random process, with, usually, assumptions of homogeneity or Gaussianity [3]-[6]. However, a number of important physical phenomena shows a clear deviation from the above assumptions. Therefore, the simulation of non-Gaussian and non-homogeneous SRF is of great importance. To accomplish this the Karhunen-Love (KL) expansion-based simulation procedure can be applied for generating both homogeneous and non-homogeneous, Gaussian and non-Gaussian SRF [1]. This technique presents two drawbacks to being used as a general simulation tool. For instance, its range of application is restricted to SRF defined on compact subsets and it also requires the computation of eigenfunctions and eigenvalues of the correlation function which is generally a difficult task.

This paper presents a simulation technique based on an approximate series representation for SRF defined on any subset of the multidimensional Euclidean space and is easily implementable in real situations. In Section 2 we introduce a suitable tool to represent approximately SRF and describe the steps involved in implementing the simulation algorithm proposed. Finally, Section 3 includes some examples illustrating the application of the proposed method to simulate some classical random models that have great relevance in applications.

2 Numerical Representation of Random Fields

Let T be any subset of the $d-$dimensional Euclidean space $\mathbb{R}^d$ and $X(\mathbf{t}), \mathbf{t} \in T$, $\mathbf{t} = (t_1, t_2, \ldots, t_d) \in T$, be a second-order SRF defined on the probability space $(\Omega, \mathcal{A}, \mathcal{P})$. Without loss of generality, we will assume $X(\mathbf{t})$ has zero mean. Moreover, the correlation function $R(\mathbf{t}, \mathbf{s})$, $\mathbf{t}, \mathbf{s} \in T$, is continuous. Let μ be a measure on $(T, \mathcal{B}_T^d)$ ($\mathcal{B}_T^d$ is the σ-algebra of $d-$dimensional Lebesgue measurable subsets of T) such that

$$\int_T R(\mathbf{t}, \mathbf{t}) d\mu(\mathbf{t}) < \infty$$

Moreover, μ can be chosen to be absolutely continuous with respect to the $d-$dimensional Lebesgue measure λ of the form

$$d\mu(\mathbf{t})/d\lambda(\mathbf{t}) = F(\mathbf{t}) \tag{1}$$

with F a non-zero a.e. $[Leb]$, non-negative and Lebesgue integrable function over T [7].

Let $\mathcal{R}_\mu$ be the Hilbert-Schmidt integral-type operator with kernel $R(\mathbf{t}, \mathbf{s})$ defined from $L_2(\mu) = L_2(T, \mathcal{B}_T^d, \mu)$ on $L_2(\mu)$ by

$$\left(\mathcal{R}_\mu \phi\right)(\mathbf{t}) = \int_T R(\mathbf{t}, \mathbf{s}) \phi(\mathbf{s}) d\mu(\mathbf{s}), \quad \mathbf{t} \in T \tag{2}$$

Let λ_i and ϕ_i be its corresponding eigenvalues and orthonormal eigenfunctions in $L_2(\mu)$.

Then we can state the following representation for $X(\mathbf{t})$,

$$X(\mathbf{t}) = \sum_{i=1}^{\infty} b_i \phi_i(\mathbf{t}), \quad \mathbf{t} \in T \tag{3}$$

*This work was supported in part by Project MTM2004-04230 of the Plan Nacional de I+D+I, Ministerio de Educación y Ciencia, Spain. This project is financed jointly by the FEDER. Department of Statistics and Operations Research, University of Jaén & Paraje Las Lagunillas, 23071, Jaén, Spain Tel/Fax: + (34) 953 21 2625/2034 Email: {aoya, jnavarro, jcruiz, rmfernan}@ujaen.es

where the series converges in the mean square sense. The random coefficients are given by

$$b_i = \int_T X(\mathbf{t})\phi_i(\mathbf{t})d\mu(\mathbf{t}) \quad \text{a.s.}$$

with $E[b_i b_j] = \lambda_i \delta_{ij}$. As a consequence of (3), we obtain a generalization of Mercer's expansion as follows

$$R(\mathbf{t},\mathbf{s}) = \sum_{i=1}^{\infty} \lambda_i \phi_i(\mathbf{t})\phi_i(\mathbf{s})$$

for all $(\mathbf{t},\mathbf{s}) \in T \times T$.

The representation (3) is optimal in the sense that the mean-square error resulting from a finite representation of the SRF is minimized [8]. Thus, this series representation synthesizes optimally the available information. However, from an experimental standpoint, the expansion (3) presents the drawback of its explicit dependence on eigenvalues and eigenfunctions of the operator $\mathcal{R}_\mu$. In most cases, closed-form eigenfunctions and eigenvalues are not available. We avoid this difficulty by using approximate eigenvalues and eigenfunctions obtained by means of a Galerkin-type numerical method to solve the operator equation (2). Specifically, we apply the Rayleigh-Ritz method (RR) [9] which is a projection approximation algorithm providing approximate solutions of the operator equation.

The RR method starts from a complete orthonormal set of functions $\{\varphi_i\}_i$ on $L_2(\mu)$. By selecting k functions $\{\varphi_i\}_{i=1}^k$, the true eigenfunctions are approximated by means of the RR eigenfunctions

$$\tilde{\phi}_i(\mathbf{t}) = \sum_{j=1}^{k} a_{ij}\varphi_j(\mathbf{t}), \quad i = 1, 2, \ldots, k$$

where the coefficients a_{ij} and the approximate eigenvalues $\left\{\tilde{\lambda}_i\right\}_{i=1}^k$ are obtained from the eigenvalue problem $\mathbf{A}\mathbf{a}_i = \tilde{\lambda}_i \mathbf{a}_i$, $i = 1, 2, \ldots, k$, with the elements of the matrix $\mathbf{A} = (A_{ij})$, $i, j = 1, \ldots, k$, given by

$$A_{ij} = \langle \mathcal{R}_\mu \varphi_i, \varphi_j \rangle_2 = \int_T \int_T R(\mathbf{t},\mathbf{s})\varphi_i(\mathbf{t})\varphi_j(\mathbf{s})d\mu(\mathbf{t})d\mu(\mathbf{s})$$

where $\langle \cdot, \cdot \rangle_2$ denotes the usual inner product in $L_2(\mu)$ and $\| \cdot \|_2$ the corresponding norm. The coefficients a_{ij} are the coordinates of the eigenvectors $\mathbf{a}_i = (a_{i1}, \ldots, a_{ik})'$, $i = 1, \ldots, k$. The convergence of the RR eigenfunctions and eigenvalues to the true ones is guaranteed by the RR method [9], $\tilde{\lambda}_i \xrightarrow{k\uparrow\infty} \lambda_i$ and $\left\|\tilde{\phi}_i(\mathbf{t}) - \phi_i(\mathbf{t})\right\|_2 \xrightarrow{k\uparrow\infty} 0$. Furthermore, $0 \le \tilde{\lambda}_i \le \lambda_i$, $\left\langle \tilde{\phi}_i, \tilde{\phi}_j \right\rangle_2 = \delta_{ij}$ (by assuming that the eigenvectors $\mathbf{a}_i$ and $\mathbf{a}_j$ are normalized) and $\left\langle \mathcal{R}_\mu \tilde{\phi}_i, \tilde{\phi}_j \right\rangle_2 = \tilde{\lambda}_i \delta_{ij}$.

The main objection to the RR eigenfunctions is that they do not necessarily converge pointwise to the true ones. For this reason we introduce a new class of approximate eigenfunctions with a stronger type of convergence toward the true ones, given by

$$\hat{\phi}_i(\mathbf{t}) = \tilde{\lambda}_i^{-1} \mathcal{R}_\mu \tilde{\phi}_i(\mathbf{t}), \qquad \mathbf{t} \in T$$

with the following convergence properties

$$\left|\phi_i(\mathbf{t}) - \hat{\phi}_i(\mathbf{t})\right| \xrightarrow{k\uparrow\infty} 0, \quad \mathbf{t} \in T$$

$$\left\|\phi_i(\mathbf{t}) - \hat{\phi}_i(\mathbf{t})\right\|_2 \xrightarrow{k\uparrow\infty} 0, \quad \mathbf{t} \in T$$

Note that the sets of approximate and RR eigenfunctions, $\left\{\hat{\phi}_i\right\}_{i=1}^k$ and $\left\{\tilde{\phi}_i\right\}_{i=1}^k$, are biorthogonal systems in $L_2(\mu)$, i.e., $\left\langle \hat{\phi}_i, \tilde{\phi}_j \right\rangle_2 = \delta_{ij}$.

The new approximate eigenfunctions allow us to obtain an approximate series representation of $X(\mathbf{t})$ as follows

$$\hat{X}_n(\mathbf{t}) = \sum_{i=1}^{n} \tilde{b}_i \hat{\phi}_i(\mathbf{t}), \quad \mathbf{t} \in T \tag{4}$$

where $n \le k$ and the random variables $\left\{\tilde{b}_i\right\}_{i=1}^n$ are given by

$$\tilde{b}_i = \int_T X(\mathbf{t})\tilde{\phi}_i(\mathbf{t})d\mu(\mathbf{t}) \quad \text{a.s.} \tag{5}$$

It can be shown that these random variables are uncorrelated, i.e. $E\left[\tilde{b}_i \tilde{b}_j\right] = \tilde{\lambda}_i \delta_{ij}$. Furthermore, the correlation function of the approximate expansion $\hat{X}_n(\mathbf{t})$ is of the form

$$\hat{R}_n(\mathbf{t},\mathbf{s}) = \sum_{i=1}^{n} \tilde{\lambda}_i \hat{\phi}_i(\mathbf{t})\hat{\phi}_i(\mathbf{s}), \quad \mathbf{t},\mathbf{s} \in T \tag{6}$$

Both series expansions (4) and (6) converge towards $X(\mathbf{t})$ and $R(\mathbf{t},\mathbf{s})$, respectively, as the length of the series representations goes to infinity.

Note that it is also possible to define an approximate expansion of the SRF by using the RR eigenfunctions, $\left\{\tilde{\phi}_i\right\}_{i=1}^n$, instead of $\left\{\hat{\phi}_i\right\}_{i=1}^n$ as follows

$$\tilde{X}_n(\mathbf{t}) = \sum_{i=1}^{n} \tilde{b}_i \tilde{\phi}_i(\mathbf{t}), \quad \mathbf{t} \in T \tag{7}$$

with $\tilde{b}_i$ the random variables in (5). However, this finite expansion provides a less accurate approximation of the SRF, $X(\mathbf{t})$, with a worse convergence than the one obtained with (4). Actually, $\hat{X}_n(\mathbf{t})$ is the projection of $X(\mathbf{t})$ onto the subspace of $L_2(\Omega, \mathcal{A}, \mathcal{P})$ spanned by the random variables $\left\{\tilde{b}_i/\tilde{\lambda}_i^{1/2}\right\}_{i=1}^n$. Hence, (4) provides the best approximation of the SRF onto such a subspace. As a consequence, the simulation results achieved with the approximate series expansion (4) perform better than those obtained by applying the representation (7) as we will illustrate by means of some numerical examples in the next section.

Finally, the following steps are involved in implementing the simulation technique proposed to obtain numerical realizations of a SRF $X(\mathbf{t})$:

1. Determine the correlation model $R(\mathbf{t},\mathbf{s})$ of the SRF, $X(\mathbf{t})$, that characterizes the spatial variability of the natural process of interest. In some practical applications the correlation model is initially known. In fact, it may be derived from experimental measurements or mathematical models [1].

2. Obtain the approximate eigenvalues and eigenfunctions corresponding to $R(\mathbf{t},\mathbf{s})$, $\tilde{\lambda}_i$ and $\tilde{\phi}_i$, by means of the RR method.

3. Generate approximate sample functions of the SRF, $X(\mathbf{t})$, using the approximate expansion (4). Note that the precision of the simulated field clearly depends on the number of terms n in the expansion (4). This finite representation involves the n random coefficients $\{\tilde{b}_i\}_i$ whose variances $\tilde{\lambda}_i$ approach the n largest exact eigenvalues λ_i of $\mathcal{R}_\mu$. An appropriate criterion for determining an adequate level of truncation n without an unnecessary excess of computation can be the following: select n in such a way that $\sum_{i=1}^{n}\tilde{\lambda}_i$ represents at least 90% of the trace of $\mathcal{R}_\mu$, $\sum_{i=1}^{\infty}\lambda_i$.

3 Simulation Results

Computer simulations have been conducted to investigate the performance of the proposed algorithm. The examples presented here are two well known SRF, the two-parameter Ornstein-Uhlenbeck and Wiener fields, which illustrate the implementation and the effectiveness of the approach proposed. Specifically, to assess the validity of the results obtained with the procedure provided and to test their convergence properties, the correlation function of the target SRF, $R(\mathbf{t},\mathbf{s})$, is compared with that of the simulated functions, $\hat{R}_n(\mathbf{t},\mathbf{s})$ and $\tilde{R}_n(\mathbf{t},\mathbf{s})$ (this is the correlation function corresponding to $\tilde{X}_n(\mathbf{t})$). It is important to point out that the examples of SRF for which the exact eigenvalues and eigenfunctions are known are limited.

3.1 Two-parameter Ornstein-Uhlenbeck field

Firstly, consider the two-parameter Ornstein-Uhlenbeck field which has been used as a benchmark model in a wide number of applications [10]. The correlation function is defined by

$$R(\mathbf{t},\mathbf{s}) = \exp(-|t_1 - s_1|)\exp(-|t_2 - s_2|) \tag{8}$$

$t_1, t_2, s_1, s_2 \in [-0.5, 0.5]$. Since the domain $[-0.5, 0.5] \times [-0.5, 0.5]$ is a compact subset of $\mathbb{R}^2$ we have selected μ as the Lebesgue measure. Its eigenfunctions and eigenvalues are of the form [8]

$$\begin{aligned} &\lambda_i = \nu_j \nu_l \\ &\phi_i(t_1,t_2) = \gamma_j(t_1)\gamma_l(t_2), \quad t_1,t_2 \in [-0.5,0.5] \end{aligned} \tag{9}$$

with $j, l = 1, 2, \ldots$ and $i = (j, l)$ a two-index, ν_j and γ_j the eigenvalues and eigenfunctions of the standard Ornstein-Uhlenbeck process.

To apply the RR method we choose k functions in the following set

$$\begin{aligned} &\{1, \sqrt{2}\cos(2\pi t_1), \sqrt{2}\cos(2\pi t_2), 2\cos(2\pi t_1)\cos(2\pi t_2), \\ &\sqrt{2}\sin(2\pi t_1), \sqrt{2}\sin(2\pi t_2), 2\cos(2\pi t_1)\sin(2\pi t_2), \\ &2\sin(2\pi t_1)\cos(2\pi t_2), 2\sin(2\pi t_1)\sin(2\pi t_2), \ldots\} \end{aligned}$$

Simulation results using $n = 100$ shown in Figure 1 are cross-sectional plots, obtained at $s_1 = 0.5$ and $t_2 = s_2 = 0$, of the correlation function (8) and the simulated functions $\hat{R}_n(\mathbf{t},\mathbf{s})$ and $\tilde{R}_n(\mathbf{t},\mathbf{s})$. It can be confirmed that the approximate function $\hat{R}_n(\mathbf{t},\mathbf{s})$ shows excellent agreement with the theoretical one compared with the behaviour of $\tilde{R}_n(\mathbf{t},\mathbf{s})$. Moreover, Figure 2 shows the sample errors committed with the two approaches, $\hat{R}_n$ and $\tilde{R}_n$, measured by $|R - \hat{R}_n|$ and $|R - \tilde{R}_n|$, respectively, with $s_1 = 0.5$, $t_2 = s_2 = 0$ and $n = 100$.

As we have indicated in the previous section, an appropriate guideline for selecting a suitable level of truncation is the examination of the percentage of the trace of the operator involved that is explained by the finite expansion. For instance, the approximate expansion $\hat{X}_n(\mathbf{t})$ for $n = 100$ can explain over 93.21% of the trace of the operator corresponding to (8) on the interval $[-0.5, 0.5]$ computed as follows

$$\sum_{i=1}^{\infty}\lambda_i = \int_{-0.5}^{0.5}\int_{-0.5}^{0.5} R(\mathbf{t},\mathbf{t})d\mathbf{t} = 1$$

3.2 Two-parameter Wiener field

The second example considered corresponds to the Wiener field which is a well known example of non-homogeneous SRF. It is also called Brownian sheet [11] or Cameron-Yeh process in engineering applications [12]. The standard two-parameter Wiener process $W(\mathbf{t})$, $\mathbf{t} = (t_1, t_2)$, defined on the domain $[0,\infty) \times [0,\infty)$ has the following correlation function

$$R(\mathbf{t},\mathbf{s}) = \min(t_1, s_1)\min(t_2, s_2), \quad t_1, t_2, s_1, s_2 \in [0,\infty) \tag{10}$$

Moreover, by (1) let μ be a measure such that $F(t_1, t_2) = \frac{1}{(1+t_1)^4(1+t_2)^4}$. Computation of eigenvalues and eigenfunctions corresponding to the Wiener field is similar to (9) where now ν_j and γ_j are the eigenvalues and eigenfunctions of the standard Wiener process.

To apply the RR method we select k functions in the following set of trigonometric functions

$$\left\{2(1+t_1)(1+t_2)\cos\left(\frac{(2i-1)\pi t_1}{2(1+t_1)}\right)\cos\left(\frac{(2j-1)\pi t_2}{2(1+t_2)}\right)\right\}_{(i,j)}$$

with $i, j = 1, 2, \ldots$

Let us observe that the approximate expansion $\hat{X}_n(\mathbf{t})$ explains over 92.06%, with $n = 225$, of the trace of the operator corresponding to the two-parameter Wiener field on the interval $[0, \infty)$ which is given by

$$\sum_{i=1}^{\infty} \lambda_i = \int_0^{\infty} \int_0^{\infty} R(\mathbf{t}, \mathbf{t}) d\mu(\mathbf{t}) = \frac{1}{36}$$

Simulation results using $n = 225$ are shown in Figure 3 which are cross-sectional plots (obtained at $s_1 = s_2 = t_2 = 10$) of the correlation function (10) and the simulated correlation function $\hat{R}_n(\mathbf{t}, \mathbf{s})$. Finally, note that the process is defined on $[0, \infty)$, but we plot the functions in the interval $[0, 30]$ because it is sufficient to assess the accuracy achieved with the proposed approach.

References

[1] Christakos, G., *Random field models in earth sciences*, Academic Press, 1992.

[2] Christakos, G., *Modern spatiotemporal geostatistics*, Oxford University Press, Oxford, 2000.

[3] Alabert, F., "The practice of fast conditional simulations through the LU decomposition of the covariance matrix," *Math Geology*, V19, N5, pp. 369-387, 1987

[4] Mantoglou, M., "Digital simulation of multivariate two- and three-dimensional stochastic processes with a spectral turning bands method," *Math Geology*, V19, N2, pp. 129-149, 1987

[5] Le Ravalec, M., Noetinger, B., Hu, L.Y., "The FFT moving average (FFT-MA) generator: an efficient numerical method for generating and conditioning Gaussian simulations," *Math Geology*, V32, N6, pp. 701-723, 2000

[6] Shinozuka, M., Deodatis, G., "Simulation of multidimensional Gaussian stochastic fields by spectral representation," *Appl Mech Rev*, V49, pp. 29-53, 1996

[7] Cambanis, S., Masry, E., "On the representation of weakly continuous stochastic processes," *Information Sci*, V3, pp. 277–290, 1971

[8] Ghanem, R., Spanos, P.D., *Stochastic finite element: a spectral approach*, Springer, New York, 1991.

[9] Chen, M., Chen, Z., Chen, G., *Approximate solutions of operator equations*, World Scientific Pub. Co., 1997.

[10] Goitía, A., Ruiz-Medina, M.D., Angulo, J.M., "Joint estimation of spatial deformation and blurring in environmental data," *Stoch Environ Res Risk Assess*, V19, pp. 1-7, 2005

[11] Adler, R.J., *The geometry of random fields*, Wiley and Sons, New York, 1980.

[12] Kailath, T., "RKHS approach to detection and estimation problems-Part I: Deterministic signals in Gaussian noise," *IEEE Trans Inform Theory*, V17, pp. 530-549, 1971

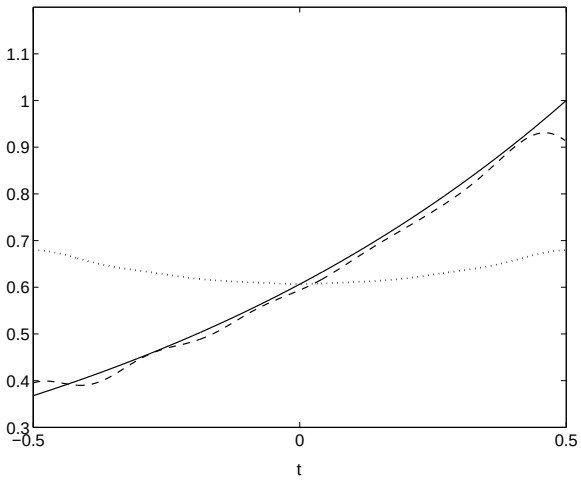

Figure 1: Comparison of R of the Ornstein-Uhlenbeck field (solid line), $\tilde{R}_{100}$ (dotted line) and $\hat{R}_{100}$ (dashed line).

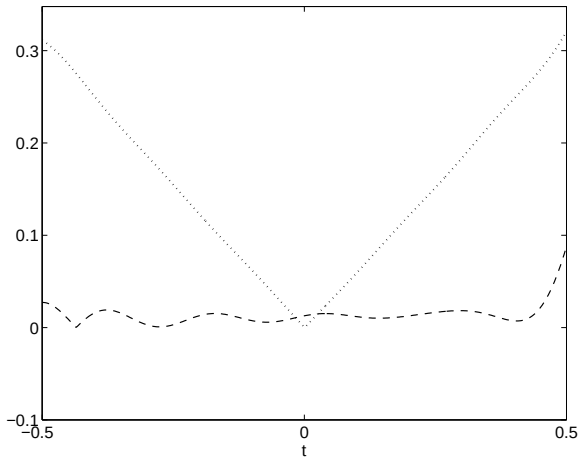

Figure 2: Comparison of sample errors with $\hat{R}_{100}$ (dashed line) and $\tilde{R}_{100}$ (dotted line) for the Ornstein-Uhlenbeck field.

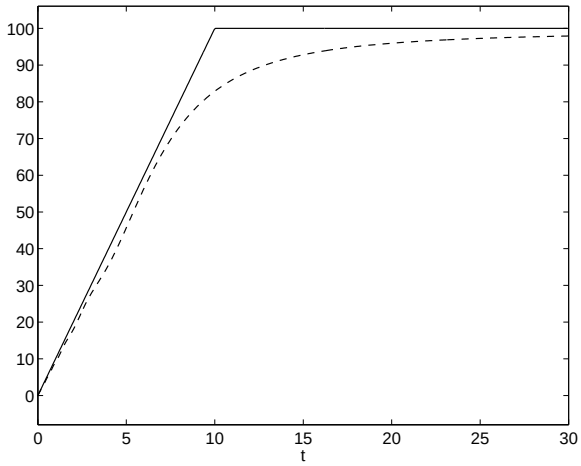

Figure 3: Comparison of R of the Wiener field (solid line) and $\hat{R}_{225}$ (dashed line).